Compressed supersymmetry at 14 TeV LHC

Biplob Bhattacherjee[*]
Kavli IPMU (WPI), The University of Tokyo, Kashiwa, Chiba 277-8583, Japan

Arghya Choudhury[†]
Department of Physical Sciences, Indian Institute of Science Education and Research—Kolkata, Mohanpur-741252, West Bengal, India

Kirtiman Ghosh[‡]
Department of Physics and Oklahoma Center for High Energy Physics, Oklahoma State University, Stillwater, Oklahoma 74078-3072, USA

Sujoy Poddar[§]
Netaji Nagar Day College, 170/436, N.S.C. Bose Road, Kolkata—700092, India
(Received 21 August 2013; published 19 February 2014)

In this work we study the collider phenomenology of a compressed supersymmetric model with the gluino ($\tilde{g}$) and the lightest neutralino ($\tilde{\chi}_1^0$). All other sparticles are assumed to be heavy. We consider gluino pair production at the 14 TeV LHC and present the mass reach of the gluino as a function of mass splitting between the gluino and the lightest neutralino. We find that the gluino mass below 1 TeV can be excluded at 95% C.L. with an integrated luminosity of 100 fb^{-1} for the extreme degenerate case where the mass separation between the gluino and the lightest neutralino is about 20 GeV. On the other hand, the lower bound on the mass of the gluino increases to 1.2–1.3 TeV if the mass splitting between the gluino and $\tilde{\chi}_1^0$ is about 200 GeV. This result shows that for a degenerate gluino, the current mass limit may approximately extend up to 400–500 GeV at the 14 TeV LHC.

DOI: 10.1103/PhysRevD.89.037702 PACS numbers: 14.80.Ly

The constrained minimal supersymmetric standard model (cMSSM) [1] is one of the supersymmetric (SUSY) models which draws much attention to the particle physics community due to its small number of parameters which make this model highly predictive. For this reason, two major collaborations of the LHC, ATLAS and CMS, have searched for the cMSSM from the very beginning of the LHC run in many different final states. In the R-parity conserving model, SUSY particles (sparticles) are produced in pairs and the lightest supersymmetric particle (LSP) must be stable. In most of the cases, the lightest neutralino ($\tilde{\chi}_1^0$), being the LSP can be a good candidate for cold dark matter. The generic signature of a SUSY search is comprised of multijets + leptons + large amount of missing transverse energy ($\not{E}_T$) which arises due to cascade decays of squarks and gluino into jets, leptons and $\tilde{\chi}_1^0$. Here $\tilde{\chi}_1^0$ is the primary source of $\not{E}_T$ which escapes the detector like neutrinos.

In cMSSM, the gluino is generally much heavier than the LSP ($m_{\tilde{g}} \sim 6 m_{\tilde{\chi}_1^0}$) and jets produced from the decay of $\tilde{g}$, i.e., $\tilde{g} \to q\bar{q}\tilde{\chi}_i^0$ are very energetic resulting in signatures having a sufficient amount of $\not{E}_T$ as well as effective mass (M_{eff}). Here M_{eff} is defined as the scalar sum of P_T of jets, P_T of leptons (wherever leptons are present) and $\not{E}_T$. These two kinematic variables ($\not{E}_T$, M_{eff}) can be efficiently used to discriminate SUSY signals from the SM backgrounds. The CMS [2] and ATLAS [3] Collaborations have searched for SUSY in the jets + leptons + $\not{E}_T$ channel and in the absence of a significant excess of signal events over the SM backgrounds, they put stringent bounds on the masses of squarks and the gluino in the framework of cMSSM using 7/8 TeV data. For example, with an integrated luminosity $(\mathcal{L}) = 20.3\ \mathrm{fb}^{-1}$, equal masses of squarks and gluino are excluded below 1.7 TeV in the cMSSM scenario from 8 TeV LHC data [3].[1]

It is to be noted that in case of a quasidegenerate mass spectrum, the P_T of jets or leptons arising from the decay of sparticles will be soft and it may even fall below the detector acceptance level. In such cases, even if the pair-production cross section of the squark and/or gluino is large, the signal may not be observed over backgrounds because of the poor acceptance. Consequently the bound on the squark/gluino mass will be drastically reduced. Attention has been paid by several authors [5–11] in this direction which basically opens up significant regions of parameter space with low squark/gluino mass. The ATLAS Collaboration has also searched for compressed SUSY scenarios assuming some

[*]biplob.bhattacherjee@ipmu.jp
[†]arghyac@iiserkol.ac.in
[‡]kirti.gh@gmail.com
[§]sujoy.phy@gmail.com

[1]Equal squark and gluino masses less than around 3 TeV can be excluded in the future [4].

specific simplified models [3,12]. In particular, if we consider a model with only $\tilde{g}$ and $\tilde{\chi}_1^0$, $m_{\tilde{g}}$ up to 500–550 GeV is excluded from the 7/8 TeV analysis by ATLAS in the case of extreme degeneracy $\Delta m(\tilde{g}-\tilde{\chi}_1^0) =$ 10–20 GeV which is consistent with the phenomenological results [5–7,9–11]. We can conclude from the above discussion that the limit on $m_{\tilde{g}}$ is considerably weaker than that with nondegenerate scenarios like cMSSM.

We know that there is a plethora of well-motivated models which do not obey the cMSSM mass hierarchy between the gauginos. For example, (i) the quasidegenerate $\tilde{g}-\tilde{\chi}_1^0$ scenario arises in some specific form of gauge-mediated SUSY breaking [13,14]. (ii) The compressed SUSY mass spectrum is an automatic outcome of supersymmetry breaking via boundary conditions in compact extra dimensions [15]. (iii) In some part of the parameter space of the pure gravity mediation model, the gluino can be nearly degenerate with the $\tilde{\chi}_1^0$ [16]. (iv) Models with a small mass difference between the gluino and LSP may be favored by precision gauge coupling unification [17]. Also the quasidegenerate gluino-neutralino scenario is well motivated from the dark matter (DM) point of view. It is well known that the annihilation of a bino-like LSP gives rise to a relic density which is too large compared to the DM relic density data measured by Planck [18]. The observed relic density can be explained if a bino-like $\tilde{\chi}_1^0$ coannihilates with a nearly degenerate gluino [19].

Initial state radiation (ISR) from the squark/gluino production process depends only on the scale of the interaction and the color structure. Hence, the hardness of ISR jets do not depend on the relative mass separation between the produced particles and the corresponding decay products in contrast to jets produced in the decay. We may expect that the ISR jets arising along with the pair production of TeV-scale squarks/gluino might be hard enough to be detected [20]. Phenomenologically, it is therefore important to study the future prospect of degenerate scenarios at the 14 TeV LHC.

In this work, we are particularly interested in the SUSY scenario with a quasidegenerate $\tilde{g}$-$\tilde{\chi}_1^0$. We consider $\tilde{g}$ pair production at the 14 TeV LHC with subsequent decay of $\tilde{g}$ into light quarks and $\tilde{\chi}_1^0$. We have focused on $2/3/4\,\text{jets} + \not{E}_T$ signatures[2] which are mainly important for compressed SUSY models. As mentioned before, for the compressed spectrum, jets mainly come from ISR. If we just generate parton-level $\tilde{g}$ pair events and pass these events through an event generator for hadronization, the ISR jets will be produced by the event generator at the time of showering. However, the ISR jet spectrum crucially depends on the factorization scale. Depending upon the choice of factorization scale, the spectrum might be harder as well as softer which induces a large amount of systematic uncertainty. Monte Carlo events generators like PYTHIA or HERWIG use different parton-showering algorithms. Depending upon the choice of generators we may get somewhat different results. In order to avoid this, we have to generate a $\tilde{g}$ pair in association with additional jets at the matrix element level. However, in order to get rid of the double counting problem at the time of parton showering we must adopt a particular matching prescription. This also reduces the systematic uncertainty coming from the different parton shower schemes although Monte Carlo event generators as a whole introduce a large amount of systematic uncertainty which cannot be removed by a matching prescription.

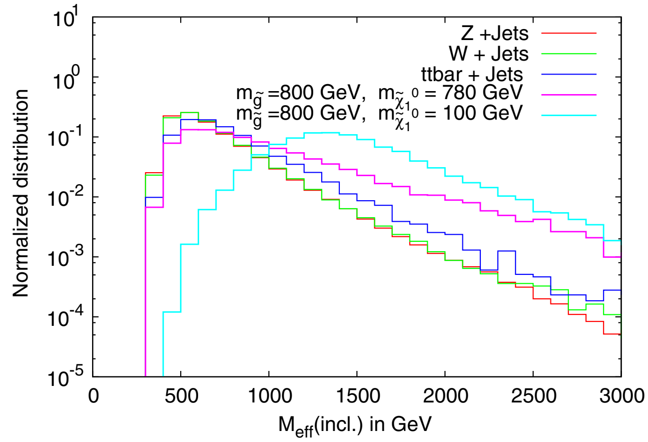

FIG. 1 (color online). Normalized M_{eff} (incl.) distribution for different SM backgrounds and SUSY benchmark points after a few nominal cuts [lepton veto, $P_T(j_1) > 130$ GeV, $P_T(j_2) > 60$ GeV and $\not{E}_T > 160$ GeV].

SUSY mass spectra and decay processes are generated by SUSY-HIT [21]. Throughout this work the LSP is assumed to be bino dominated and all SUSY particles except $\tilde{g}$ and $\tilde{\chi}_1^0$ are set beyond the reach of the 14 TeV LHC. The DM relic density is computed by using MicrOMEGAs [22] for our scenario. We have used MadGraph 5 [23] for generating both signal events and SM backgrounds at the parton level. For signal events we have generated $\tilde{g}\tilde{g}$ and $\tilde{g}\tilde{g}$ plus one additional jet at the parton level. Dominant backgrounds for our analysis are $Z+\text{jets}$, $W+\text{jets}$ and $t\bar{t}+\text{jets}$.[3] W/Z backgrounds are generated up to an additional four jets and for $t\bar{t}$ events we have considered up to two jets. Subsequently signal and background events are passed through PYTHIA [24] for showering, decay, hadronization, etc. For matching purposes we have used the MLM [25] prescription as implemented in MadGraph 5 for both signal and backgrounds. Finally the events are fed to the fast detector simulator

[2]Monojet plus $\not{E}_T$ is also a viable signal of degenerate gluino production. However, 7/8 TeV results [9,10] show that it is weaker than the conventional $2/3\,\text{jets} + \not{E}_T$ searches.

[3]QCD multijets and electroweak gauge boson pairs may be considered as potential backgrounds. However, after the inclusion of all cuts discussed in Table I, these backgrounds turn out to be negligibly small and hence they are not included in our analysis.

TABLE I. Selection criteria considered in our analysis at the 14 TeV LHC and upper limits on the number of BSM events. The SRB-M, SRB-T, and SRC-T signal regions are taken from Ref. [3] and signal regions are denoted by the same convention as that used by ATLAS. The SRA-OT, SRB-OT, SRC-OM, and SRC-OT signal regions are obtained by optimization of cuts. O, T, M denote optimized, tight and medium, respectively. Leptons are vetoed in all of the signal regions. $M_{\rm eff}(N_j)$ is constructed from only the leading N jets (indicated in parentheses in the second row) and E_T. ** For SRA-OT, the $\delta\phi(\text{jet}_i, E_T)_{\rm min}$ cut is applied for $i = 1$ to 3 if $P_T(j_3) > 40$ GeV.

	Channel						
Cuts	SRA-OT (2j)	SRB-M (3j)	SRB-T (3j)	SRB-OT (3j)	SRC-T (4j)	SRC-OM (4j)	SRC-OT (6j)
E_T [GeV] $>$	200	160	160	200	160	200	200
$P_T(j_1)$ [GeV] $>$	200	130	130	150	130	150	150
$P_T(j_2)$ [GeV] $>$	100	60	60	80	60	80	80
$P_T(j_3)$ [GeV] $>$	...	60	60	80	60	80	80
$P_T(j_4)$ [GeV] $>$	...	...	...	...	60	80	80
$\delta\phi(\text{jet}_i, E_T)_{\rm min}$	0.4 $(i = 1, 2)$**	0.4 $(i = 1, 2, 3)$	0.4 $(i = 1, 2, 3)$	0.4 $(i = 1, 2, 3)$		0.4$(i = [1, 2, 3])$ 0.2($P_T > 40$ GeV jets)	
$E_T/M_{\rm eff}(N_j) >$	0.4	0.3	0.4	0.4	0.25	0.4	0.3
$M_{\rm eff}$ (incl.) [GeV] $>$	2400	1800	2200	2400	2200	2200	2400
$Z +$ jets [fb]	4.0	18.4	3.9	1.8	2.8	0.66	0.9
$W +$ jets [fb]	1.15	8.6	1.2	0.6	1.2	0.15	0.4
$t\bar{t} +$ jets [fb]	0.25	4.3	0.3	0.1	0.4	0.12	0.2
Total SM background [fb]	5.4	31.3	5.4	2.5	4.4	0.93	1.5
Upper limit on $N_{\rm BSM}$ at 95% C.L. Sys. Un $= 20\%$, $\mathcal{L} = 30$ fb^{-1}	59	381	68	35	57	17	23
Upper limit on $N_{\rm BSM}$ at 95% C.L. Sys. Un $= 10\%$, $\mathcal{L} = 100$ fb^{-1}	116	636	116	59	97	27	39

package DELPHES [26] for object reconstructions.[4] For signal, next-to-leading-order (NLO) cross sections are obtained from PROSPINO 2.1 [27]. For the $t\bar{t}$ background we have used an NLO cross section [28]. The K factors for electroweak processes (W/Z backgrounds) are generally small, ∼1.15–1.20 [29]. Instead of an explicit computation of the K factors for those processes, we conservatively assume $K = 1.2$ for W/Z productions.

The crucial variables described previously, used for the SUSY search are E_T and $M_{\rm eff}$. It is thus important to study the shape of these distributions for degenerate SUSY and compare it with SM backgrounds. In Fig. 1 we have illustrated the normalized $M_{\rm eff}$ (incl.) distribution after some nominal cuts where $M_{\rm eff}$ (incl.) is defined as the scalar sum of E_T and P_T of all jets satisfying $P_T > 40$ GeV. For illustration, we choose two benchmark points, one with large Δm ($m_{\tilde{g}} = 800$ GeV, $m_{\tilde{\chi}_1^0} = 100$ GeV) and another with small mass splitting ($m_{\tilde{g}} = 800$ GeV, $m_{\tilde{\chi}_1^0} = 780$ GeV). Figure 1 shows a clear distinction between signal and background distributions for the nondegenerate scenario as expected. For the degenerate benchmark point, $M_{\rm eff}$ (incl.) peaks at a lower value similar to SM backgrounds. However, for higher values of $M_{\rm eff}$ (incl.) SM backgrounds fall rapidly in comparison to both SUSY benchmark points and a strong cut on $M_{\rm eff}$ (incl.) (e.g., $>$ 1.5 TeV) which may be used to probe degenerate SUSY. It is also clear from Fig. 1 that the above-mentioned cut is more effective for the nondegenerate spectrum. Similarly, the E_T distribution also has the same behavior. We should note that the discovery of a SUSY signal depends on the tail of the background distributions and care should be taken to generate the tail which consists of very low-probability events. To verify the stability of our result we have also generated a sufficient number of events (∼100 fb^{-1}) by applying a $M_{\rm eff}$ (incl.) cut at the parton level using MADGRAPH. We have checked that the backgrounds estimated using these two methods [with and without the parton-level $M_{\rm eff}$ (incl.) cut] are quite consistent with each other.

Motivated by the above discussion we study the prospect of a degenerate $\tilde{g}$ search at the early run of the 14 TeV LHC. We vary the mass difference between $\tilde{g}$ and $\tilde{\chi}_1^0$ from 20 to 200 GeV for $m_{\tilde{g}}$ in the range (550–1500) GeV and by changing $\Delta m = (m_{\tilde{g}} - m_{\tilde{\chi}_1^0})$, we present the expected future limit in the $m_{\tilde{g}} - \Delta m$ plane. For analysis we choose three different strategies described below.

Strategy A: The ATLAS Collaboration has studied the prospect of a SUSY search in the 2–4 jets $+ E_T$ channel at the 14 TeV run [30]. Excepting the variation of $M_{\rm eff}$ cuts not considered by the ATLAS Collaboration, we closely follow their analysis.

Strategy B: We adopt the cuts used in the latest ATLAS 8 TeV analysis in the jets $+ 0l + E_T$[5] search channels with

[4]Jets are reconstructed using an anti-k_t algorithm with $R = 0.4$.

[5]Events with an isolated electron/muon with $P_T > 10$ GeV are rejected.

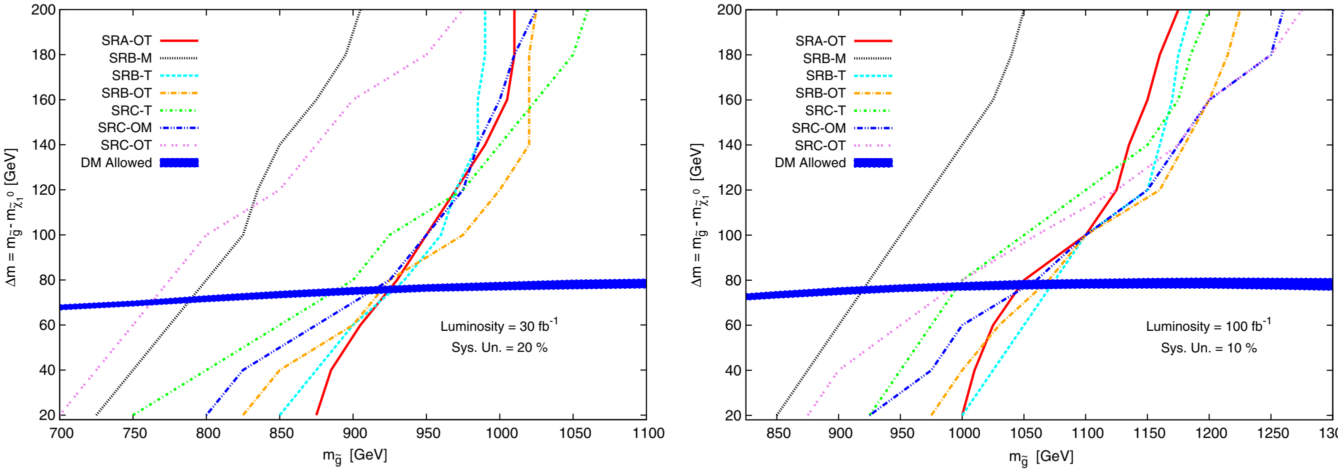

FIG. 2 (color online). 95% C.L. exclusion limit in the $m_{\tilde{g}}$ vs $\Delta m = m_{\tilde{g}} - m_{\tilde{\chi}_1^0}$ plane with an integrated $\mathcal{L} = 30$ (top) and 100 fb^{-1} (bottom) assuming systematic uncertainties of 20% and 10%, respectively. Exclusion lines correspond to the seven signal regions as described in Table I. The shaded (blue) region represents the 3σ band of the allowed DM relic density measured by the Planck Collaboration.

$\mathcal{L} = 20.3$ fb^{-1} [3]. As our signal consists of low jet multiplicities (mainly ISR jets), we do not consider signal regions with jet multiplicity greater than 4. Details of the cuts used in our analysis are presented in Table I.

It is found that better results are obtained using Strategy B compared to Strategy A. For this reason we do not further discuss the old ATLAS analysis (Strategy A).

Srategy C: Since Strategy B is optimized for the 8 TeV analysis, we expect more stronger cuts on variables for 14 TeV. Therefore, in order to enhance the significance, we try to optimize different variables like the P_T of jets, E_T, M_{eff} (incl.), $E_T/M_{\text{eff}}(N_j)$, etc. for our 14 TeV analysis. We define more than 200 different possible combinations of cuts and we choose four sets of cuts which give the best results for the degenerate scenario as described in Table I. In Table I SRA-OT stands for the optimized set of cuts for the two-jet signal region with T denoting a tight cut on M_{eff} (incl.). Other notations have similar meanings, defined in Table I.

Seven signal regions that are relevant for the search for a degenerate gluino are described in Table I. Contributions of individual SM backgrounds after the final cut are also shown in Table I. We can see from Table I that the dominant backgrounds arise from $Z(W)$ + jets production followed by $Z \to \nu\nu$ and $W \to l\nu$. The first one is the irreducible background for the jets $+ 0l + E_T$ signature whereas the second one contributes only when the lepton is not reconstructed.

We have computed the upper limit on the number of SUSY events (N_{BSM}) for an integrated $\mathcal{L} = 30$ and 100 fb^{-1} assuming systematic uncertainties of 20% and 10%, respectively, using the Bayesian method at 95% C.L. The last two rows of Table I represent these numbers.

In Fig. 2 we present the exclusion limits on the gluino mass in the $m_{\tilde{g}}$ vs $m_{\tilde{g}} - m_{\tilde{\chi}_1^0}$ plane using seven signal regions defined in Table I with $\mathcal{L} = 30$ fb^{-1} and a systematic uncertainty = 20%. The SRA-OT signal region gives the best limit: $m_{\tilde{g}} > 875$ GeV for te extreme degenerate scenario ($\Delta m = 20$ GeV) and for $\Delta m = 200$ GeV we obtain $m_{\tilde{g}} > 1050$ GeV using the signal region SRC-T. Again with an increased $\mathcal{L} = 100$ fb^{-1} and less systematic uncertainties (10%), SRB-T or SRB-OT gives the best exclusion limit on $m_{\tilde{g}}$ (>1 TeV) for $\Delta m = 20$ GeV. For $\Delta m = 200$ GeV SRC-OT excludes $m_{\tilde{g}}$ below 1275 GeV.

Here we recall that the mass limit depends significantly on the systematic uncertainty and the bounds presented in Fig. 2, assuming that a 10% uncertainty for $\mathcal{L} = 100$ fb^{-1} may be optimistic. It is a very challenging task to reduce the systematic uncertainty to such a small value in future LHC runs and it is thus important to study the sensitivity of limits on the systematic uncertainty. If we consider a high-luminosity ($\mathcal{L} = 300$ fb^{-1}) option with a 20% systematic uncertainty, the gluino mass limit is expected to be about 925 GeV, whereas this limit is reduced to about 800 GeV for a 30% systematic uncertainty. Assuming a systematic uncertainty = 20% and $\mathcal{L} = 300$ fb^{-1}, the 5σ discovery reach of the gluino is just 725 GeV for extreme degeneracy, which is close to the current LHC exclusion limit. Although, our main focus is to search for a degenerate gluino, the results, presented in this paper can be directly used for degenerate squark production, dark matter searches and other degenerate new physics scenarios like the minimal version of the universal extra dimension model [31].

Conclusion: In this paper we have considered a scenario with a gluino as the next-to-lightest supersymmetric particle (NLSP) and the mass difference between $\tilde{g}$ and $\tilde{\chi}_1^0$ is smaller compared to the conventional cMSSM model. This type of scenario can be realized in various SUSY-breaking mechanisms and $\tilde{g}$-$\tilde{\chi}_1^0$ coannihilation can explain the observed DM relic density of the Universe. Moreover, the present bound on $m_{\tilde{g}}$, obtained from LHC 7/8 TeV data is rather weak ($m_{\tilde{g}} > 500$–550 GeV). It is thus very important to study the future search prospects of such a scenario as there is no detailed phenomenological work in this direction to date for the 14 TeV LHC. The signal consists of a small number of jets (dominantly ISR jets), a moderate amount of E_T and $M_{\rm eff}$ (incl.) making the signal challenging to discover over huge SM backgrounds. We have investigated the discovery reach of jets $+ 0l + E_T$ channels for the quasidegenerate gluino NLSP and neutralino LSP scenario at the 14 TeV LHC with an integrated luminosity up to 100 fb^{-1} using optimized cuts (presented in Table I). We have found that it is possible to exclude $m_{\tilde{g}}$ up to 1 TeV for the extreme degenerate case at 95% C.L. For the moderately degenerate case ($\Delta m = 200$ GeV), the exclusion limit on $m_{\tilde{g}}$ may reach up to (1.2–1.3) TeV at 95% C.L. in the near future. Although we have investigated the degenerate gluino case, this analysis is more generic in nature and it can be applied to any other new physics searches using jets (+0l) plus a small or moderate amount of E_T in the final state.

ACKNOWLEDGMENTS

The work of B. B. is supported by World Premier International Research Center Initiative (WPI Initiative), MEXT, Japan. The work of K. G. is supported by US Department of Energy, Grant Number DE-FG02-04ER41306.

[1] G. L. Kane, C. F. Kolda, L. Roszkowski, and J. D. Wells, Phys. Rev. D **49**, 6173 (1994).
[2] S. Chatrchyan *et al.* (CMS Collaboration), Eur. Phys. J. C **73**, 2568 (2013).
[3] ATLAS Collaboration, Report No. ATLAS-CONF-2013-047.
[4] ATLAS Collaboration, Report No. ATL-PHYS-PUB-2013-002.
[5] D. S. Alves, E. Izaguirre, and J. G. Wacker, Phys. Lett. B **702**, 64 (2011).
[6] T. J. LeCompte and S. P. Martin, Phys. Rev. D **84**, 015004 (2011).
[7] T. J. LeCompte and S. P. Martin, Phys. Rev. D **85**, 035023 (2012).
[8] E. Alvarez and Y. Bai, J. High Energy Phys. 08 (**2012**) 003.
[9] H. K. Dreiner, M. Kramer, and J. Tattersall, Europhys. Lett. **99**, 61001 (2012).
[10] B. Bhattacherjee and K. Ghosh, arXiv:1207.6289.
[11] H. Dreiner, M. Krmer, and J. Tattersall, Phys. Rev. D **87**, 035006 (2013).
[12] G. Aad *et al.* (ATLAS Collaboration), Phys. Rev. D **87**, 012008 (2013).
[13] S. Raby, Phys. Lett. B **422**, 158 (1998).
[14] A. Mafi and S. Raby, Phys. Rev. D **63**, 055010 (2001).
[15] H. Murayama, Y. Nomura, S. Shirai, and K. Tobioka, Phys. Rev. D **86**, 115014 (2012).
[16] K. Nakayama and T. T. Yanagida, Phys. Lett. B **722**, 107 (2013).
[17] S. Krippendorf, H. P. Nilles, M. Ratz, and M. W. Winkler, Phys. Rev. D **88**, 035022 (2013).
[18] P. Ade *et al.* (Planck Collaboration), arXiv:1303.5076.
[19] S. Profumo and C. Yaguna, Phys. Rev. D **69**, 115009 (2004).
[20] J. Alwall, K. Hiramatsu, M. M. Nojiri, and Y. Shimizu, Phys. Rev. Lett. **103**, 151802 (2009).
[21] A. Djouadi, M. Muhlleitner, and M. Spira, Acta Phys. Pol. B **38**, 635 (2007).
[22] G. Belanger, F. Boudjema, A. Pukhov, and A. Semenov, Comput. Phys. Commun. **149**, 103 (2002).
[23] J. Alwall, M. Herquet, F. Maltoni, O. Mattelaer, and T. Stelzer, J. High Energy Phys. 06 (**2011**) 128.
[24] T. Sjostrand, S. Mrenna, and P. Z. Skands, J. High Energy Phys. 05 (**2006**) 026.
[25] M. L. Mangano, M. Moretti, F. Piccinini, and M. Treccani, J. High Energy Phys. 01 (**2007**) 013.
[26] S. Ovyn, X. Rouby, and V. Lemaitre, arXiv:0903.2225.
[27] W. Beenakker, R. Hopker, and M. Spira, arXiv:hep-ph/9611232.
[28] "Hathor-hadronic top and heavy quarks cross section calculator," https://twiki.cern.ch/twiki/bin/view/Sandbox/CrossSectionsCalculationTool.
[29] S. Catani, L. Cieri, G. Ferrera, D. de Florian, and M. Grazzini, Phys. Rev. Lett. **103**, 082001 (2009).
[30] G. Aad *et al.* (ATLAS Collaboration), arXiv:0901.0512.
[31] T. Appelquist, H.-C. Cheng, and B. A. Dobrescu, Phys. Rev. D **64**, 035002 (2001).